Universal fluctuations in the tail probability for $d = 2$ random walks in space-time random environments

Franscesca Ark, Jacob B. Hass, and Eric I. Corwin
Department of Physics and Materials Science Institute, University of Oregon, Eugene, Oregon 97403, USA

(Received 29 August 2025; accepted 22 January 2026; published 9 February 2026)

Many diffusive systems involve correlated random walkers due to a shared environment. Such systems can be modeled as random walks in random environments (RWRE). These models differ from classical diffusion in the behavior of the extremes—the walkers that move the fastest or farthest. In spatial dimension $d = 1$, RWRE models have been well studied numerically and analytically and exhibit universal behavior in the Kardar-Parisi-Zhang universality class. Here we study discrete lattice RWRE models in $d = 2$. We find that the tail probability exhibits a different universal scaling form, which is nevertheless characterized by the same coefficient, λ_{ext}, as in the $d = 1$ case. We observe a critical scaling regime for fluctuations in the tail probability at positions that scale linearly in time.

DOI: 10.1103/k6rd-wwlx

I. INTRODUCTION

The random walk in a random environment (RWRE) model takes into account the shared environment in which particles diffuse, unlike classical diffusion which treats particles as independent and identical [1–3]. The shared environment is important to the behavior of the extremes: those that travel the fastest or farthest. In many biological and physical systems, such as sperm cells searching for eggs [4,5], calcium ions traveling across dendritic spinal structures [6], and contagions spreading through a population [7–9], the meaningful action is accomplished by the first, or first handful, of arriving agent(s). Studies of diffusion in random environments have primarily focused on models in $d = 1$ [10–15] or random environments that are quenched with respect to time [16–20]. Analytical and numerical results show that RWRE models in dimension $d = 1$ fall into the Kardar-Parisi-Zhang (KPZ) universality class [11,13–15,21–26] (an analogous link has been conjectured for $d > 1$ [21]), which describes growth processes of random media [27], turbulent liquid crystals [28,29], and directed polymers [30,31]. However, diffusion across surfaces and through volumes is physically relevant, and thus it is necessary to understand diffusion in shared environments in $d > 1$.

To study diffusion in shared environments, we consider a two-dimensional discrete lattice model. We model the shared environment as a random forcing field affecting the nearest-neighbor transition probabilities for every site $\vec{x}$ for all times t (see Fig. 1, top). These transition probabilities are independently sampled from the same underlying distribution, ν. The probability to be at site $\vec{x}$ at time t can then be expressed by a master equation based on the probability at neighboring sites at time $t - 1$ [Eq. (2)]. The time- and space-averaged environment sets the diffusion coefficient D [Eq. (4)], which controls the motion of typical particles. We define an extreme diffusion coefficient, D_{ext}, which controls the statistics of the extremes of the distribution. Quantitatively, D_{ext} is defined as the variance of a single jump averaged over all environments [see Eq. (5)]. Qualitatively, D_{ext} encodes the stickiness, the degree to which particles happen to arrive at the same site at the same time subsequently move along the same trajectory. Thus, $D_{\text{ext}} \to 0$ reduces to classical diffusion, wherein trajectories are independent, and $D_{\text{ext}} \to D$ corresponds to totally sticky motion, wherein particles move in lockstep for all time. The underlying distributions we study are chosen to interpolate between these different behaviors. We study the extreme behavior by measuring the tail probability the net probability past a circle of some radius r (see Fig. 1, bottom, and Fig. 2). We show that the parameter D_{ext} is sufficient to universally describe the first-order tail probability (see Fig. 3) and its fluctuations over all distributions ν (see Fig. 4). These fluctuations flow to a constant when $r \propto t$ [see Eq. (8) and Fig. 4], in contrast to the $d = 1$ case where fluctuations flow to a constant when $r \propto t^{3/4}$.

II. RWRE MODEL DESCRIPTION

We consider random environments in which the probability of moving in each cardinal direction changes at each time and each location, as in a random forcing field. Our model is visualized in Fig. 1 (top).

Let $\boldsymbol{n} = \{\hat{x}, \hat{y}, -\hat{x}, -\hat{y}\}$ denote the set of cardinal directions. Let ν be a probability distribution on the space of probability distributions on $\boldsymbol{n}$. We denote $\mathbb{E}_\nu[\bullet]$, $\text{Var}_\nu[\bullet]$ to be the expectation value and variance over all samples of ν. We define the environment $\boldsymbol{\xi} = \{\xi_{\vec{x},t} : \vec{x} \in \mathbb{Z}^2, t \in \mathbb{Z}_{\geqslant 0}\}$, where $\xi_{\vec{x},t}$ is a probability distribution on $\boldsymbol{n}$, independently sampled according to ν, for each lattice site $(\vec{x}, t)$. We refer to $\xi_{\vec{x},t}$ as the jump distribution of a random walk. At each space-time pair, the direction of the jump is chosen randomly according to the jump distribution, $\xi_{\vec{x},t}$. Since every jump distribution is only defined on the cardinal directions, $\boldsymbol{n}$, we only consider nearest-neighbor random walks. We also only consider environments with no net drift and equal diffusion coefficients

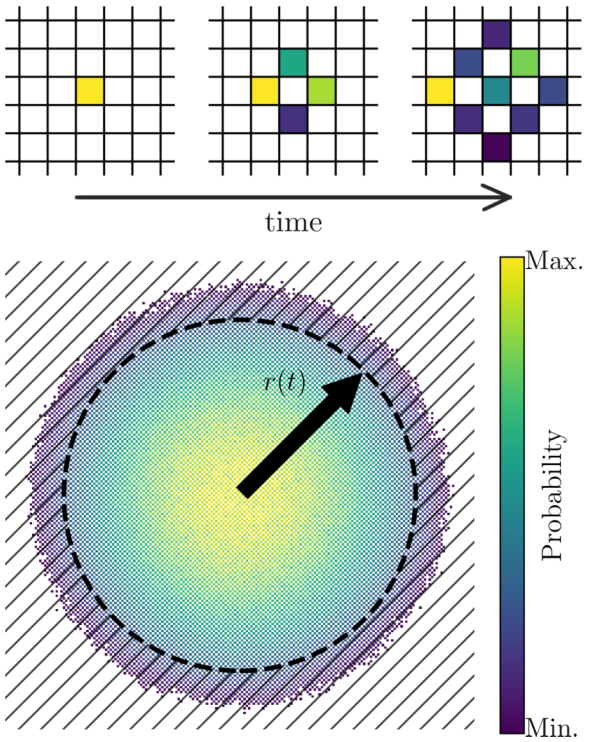

FIG. 1. Illustration of the space-time evolution of the probability mass function defined in Eq. (2) and the definition of the tail probability $\mathbb{P}^{\boldsymbol{\xi}}(|\vec{S}(t)| \geqslant r)$ for an RWRE in $d = 2$. The color indicates the relative probability. Top: Probability mass function for $t = 0, 1, 2$. We begin with unit probability at the origin. We generate four random numbers between [0,1] from some distribution, assign each of them to a direction, then move the probability from the origin to each nearest-neighbor according to those random numbers. At the next time step, for each site with nonzero probability, a set of random numbers is independently drawn from the same distribution, and probability is moved to that site's nearest neighbors.Bottom: Probability mass function at time $t = 500$ for a single $\boldsymbol{\xi}$. We sum the probability past a circle of radius r (hatched area) to find the tail probability $\mathbb{P}^{\boldsymbol{\xi}}(|\vec{S}(t)| \geqslant r)$.

along the x and y directions, such that $\sum_{\hat{n}\in\boldsymbol{n}} \mathbb{E}_\nu[\xi(\hat{n})]\hat{n} = \vec{0}$, and $\mathbb{E}_\nu[\xi(\hat{n})] = 1/4$ for all $\hat{n}$ in $\boldsymbol{n}$. Note, here and below we drop the subscript on $\mathbb{E}_\nu[\xi(\bullet)]$ since all $\xi_{\vec{x},t}$ are independent and identically distributed (i.i.d.) according to ν.

Let $\vec{S}(t) \in \mathbb{Z}^2$ denote a random walk starting at the origin such that $\vec{S}(0) = \vec{0}$. Let $\mathbb{P}^{\boldsymbol{\xi}}$ denote the probability measure of a random walk in the environment $\boldsymbol{\xi}$, and let $\mathbb{E}^{\boldsymbol{\xi}}[\bullet]$ and $\mathrm{Var}^{\boldsymbol{\xi}}[\bullet]$ be the corresponding expectation value and variance. In the environment $\boldsymbol{\xi}$, the probability of a random walk at $\vec{S}(t) = \vec{x}$ transitioning to $\vec{S}(t+1) = \vec{x} + \hat{n}$ is

$$\mathbb{P}^{\boldsymbol{\xi}}(\vec{S}(t+1) = \vec{x} + \hat{n} \mid \vec{S}(t) = \vec{x}) = \xi_{\vec{x},t}(\hat{n}) \tag{1}$$

for $\hat{n} \in \boldsymbol{n}$. Then the probability of a random walk being at site $\vec{x}$ at time t, $\mathbb{P}^{\boldsymbol{\xi}}(\vec{S}(t) = \vec{x})$, obeys the recursion relation

$$\mathbb{P}^{\boldsymbol{\xi}}(\vec{S}(t+1) = \vec{x}) = \sum_{\hat{n}\in\boldsymbol{n}} \mathbb{P}^{\boldsymbol{\xi}}(\vec{S}(t) = \vec{x} - \hat{n})\xi_{\vec{x}-\hat{n},t}(\hat{n}) \tag{2}$$

with the initial condition $\mathbb{P}^{\boldsymbol{\xi}}(\vec{S}(0) = \vec{0}) = 1$.

A. Extreme diffusion coefficient

We define

$$\lambda_{\mathrm{ext}} := \frac{1}{2}\frac{D_{\mathrm{ext}}}{D - D_{\mathrm{ext}}}, \tag{3}$$

where

$$D := \frac{1}{4}\sum_{\hat{n}\in\boldsymbol{n}} (\hat{n}\cdot\hat{n})\mathbb{E}_\nu[\xi(\hat{n})] \tag{4}$$

is the diffusion coefficient of a random walk in the average environment. Since we only consider environments where $\mathbb{E}_\nu[\xi(\hat{n})] = 1/4$ for all $\hat{n} \in \boldsymbol{n}$, then $D = 1/4$. We define D_{ext}, the *extreme diffusion coefficient*, as

$$\begin{aligned} D_{\mathrm{ext}} :&= \tfrac{1}{4}\mathrm{Var}_\nu[\mathbb{E}^{\boldsymbol{\xi}}[\vec{Y}]] \\ &= \tfrac{1}{4}\mathbb{E}_\nu[(\mathbb{E}^{\boldsymbol{\xi}}[\vec{Y}])^2] - \tfrac{1}{4}\mathbb{E}_\nu[\mathbb{E}^{\boldsymbol{\xi}}[\vec{Y}]]^2, \end{aligned} \tag{5}$$

where $\vec{Y}$ is a single step in a random walk, drawn from $\xi_{\vec{x},t}$. Thus we see $\mathbb{E}^{\boldsymbol{\xi}}[\vec{Y}] = \sum_{\hat{n}\in\boldsymbol{n}} \hat{n}\xi_{\vec{x},t}(\hat{n})$. Since we only consider net drift free systems, $\mathbb{E}_\nu[\mathbb{E}^{\boldsymbol{\xi}}[\vec{Y}]] = \vec{0}$, so we drop the second term in Eq. (5). Thus, D_{ext} simplifies to

$$D_{\mathrm{ext}} = \frac{1}{4}\mathbb{E}_\nu\left[\left(\sum_{\hat{n}_1\in\boldsymbol{n}} \hat{n}_1\xi_{\vec{x},t}(\hat{n}_1)\right)\cdot\left(\sum_{\hat{n}_2\in\boldsymbol{n}} \hat{n}_2\xi_{\vec{x},t}(\hat{n}_2)\right)\right]. \tag{6}$$

Note that we have defined λ_{ext} and D_{ext} as the $d = 2$ extension of their definition in studies of the $d = 1$ model [14]. In the case of $d = 1$, a single step of a random walk is a scalar quantity; therefore, $D_{\mathrm{ext}} = \frac{1}{2}\mathbb{E}_\nu[(\sum_i \xi_{x,t}(i)i)^2]$. To appropriately generalize this definition to $d = 2$, a single step becomes a vector, and thus we take the dot product to compute the variance.

B. Choices of distribution

We now describe the choices of ν that we implement numerically. These distributions include environments in which random walks stick to one another, and environments which are homogeneous, as in the case of classical diffusion. Note that the homogeneous environment, which returns classical diffusion, is the one where $\xi(\hat{n}) = 1/4$ for all $\hat{n} \in \boldsymbol{n}$, called the *simple symmetric random walk* (SSRW). These choices probe the universality of $d = 2$ RWRE models.

(1) *The Dirichlet distribution.* Let $\xi(\hat{n}) = X_{\hat{n}}/(\sum_{\hat{n}} X_{\hat{n}})$ for $\hat{n} \in \boldsymbol{n}$, where $X_{\hat{n}}$ are independent Gamma random variables with shape $\alpha \in \mathbb{R}_{>0}$ and rate $\beta = 1$ such that $X_{\hat{n}} = x$ with probability density $x^{\alpha-1}e^{-x}/\Gamma(\alpha)$, where $\Gamma(x)$ is the Gamma function. This distribution is completely determined by the parameter α. As $\alpha \to \infty$, $\xi(\hat{n}) \to 1/4$ for all $\hat{n} \in \boldsymbol{n}$, so the SSRW is obtained. As $\alpha \to 0$, $\xi(\hat{n}) = 1$ for one $\hat{n} \in \boldsymbol{n}$ and $\xi(\hat{n}) = 0$ otherwise. This corresponds to a perfectly sticky environment so that the jump distribution is concentrated in one direction. As the Dirichlet distribution is the multiterm generalization of the Beta distribution, it is a natural choice to explore the full range between SSRW and perfectly sticky. In this work we choose $\alpha_i = (\sqrt{10})^i/\sqrt{1000}$ for $i = 0, 1, 2, 3, 4, 5, 6$.

(2) *Log normal.* Let $\xi(\hat{n}) = X_{\hat{n}}/(\sum_{\hat{n}} X_{\hat{n}})$, where $X_{\hat{n}}$ are independent log-normal random variables with location $\mu = 0$ and scale $\sigma = 1$ such that $X_{\hat{n}} = x$ with probability density

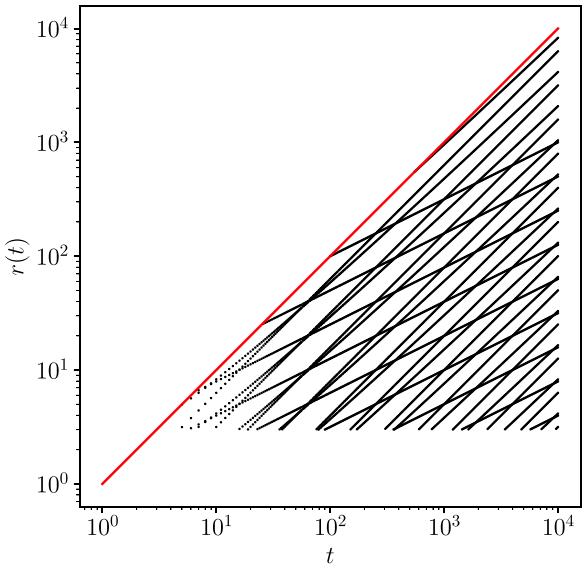

FIG. 2. The set of radii, r, vs time, t, at which we measure $\mathbb{P}^{\boldsymbol{\xi}}(|\vec{S}(t)| \geqslant r)$. The red line shows $r = t$.

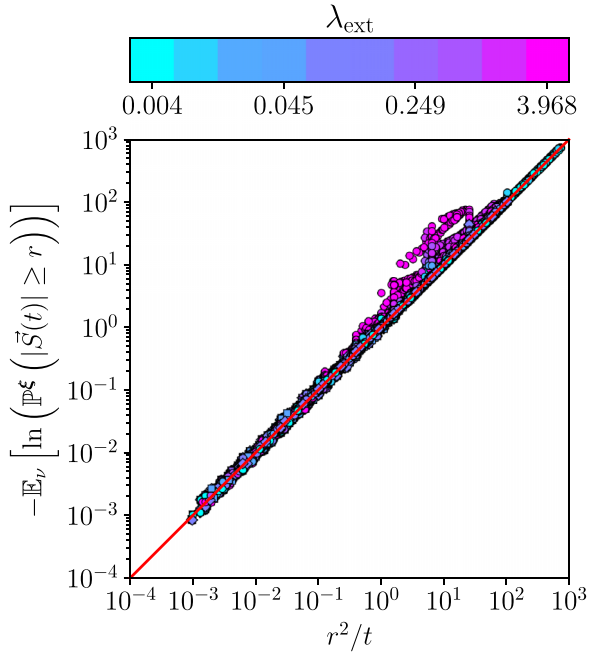

FIG. 3. Collapse of the negative mean, with respect to ν, of the natural log of the tail probability to a master curve when plotted against the Gaussian prediction r^2/t. Equation (7) is plotted as a red line, showing the validity of this prediction. The color of each data point indicates the value of λ_{ext} from 0.004 (cyan) to 4 (pink). Marker shape indicates choice of ν: Dirichlet (circles), random-delta (triangles), corner distribution (squares).

$(e^{-(\ln x)^2/2})/(x\sqrt{2\pi})$. The log-normal distribution was chosen as a nonpathological but non-Dirichlet distribution to test whether the shape of the distribution mattered for a fixed D and D_{ext}.

(3) *Random Delta.* Let $\vec{X}_1$ and $\vec{X}_2$ be two random vectors uniformly sampled from $\boldsymbol{n}$ without replacement, and set $\xi(\vec{X}_1) = \xi(\vec{X}_2) = 1/2$ and $\xi(\hat{n}) = 0$ otherwise. The random-delta distribution is a pathological case in the sense that the magnitude is fixed and randomness only enters in the form of the imposing only two directions.

(4) *Corner.* Let X_1 and X_2 be independent uniform random variables on the interval [0,1], and set $\xi(\hat{y}) = X_1/2$, $\xi(\hat{x}) = (1 - X_1)/2$ and similarly, $\xi(-\hat{x}) = X_2/2$, $\xi(-\hat{y}) = (1 - X_2)/2$. The corner distribution is a second pathological case in the sense that this distribution breaks spatial symmetry while still respecting the zero net drift and isotropy conditions.

III. NUMERICAL MEASUREMENTS

We study the statistics of the tail probability, $\mathbb{P}^{\boldsymbol{\xi}}(|\vec{S}(t)| \geqslant r)$, where $|\vec{x}|$ is the L^2 norm of the vector $\vec{x}$. This is the probability that a random walk in a given random environment is past a circle with radius r. A visualization of the definition of the tail probability is shown in Fig. 1 (bottom). The tail probability is relevant to the behavior of extreme particles, and its $d = 1$ analog has been studied extensively for the RWRE model [11,15,21,22,24,25]. As in those works, we look at the statistics of $\ln(\mathbb{P}^{\boldsymbol{\xi}}(|\vec{S}(t)| \geqslant r))$. At each measurement time t, logarithmically spaced from $t = 1$ to $t = 10\,000$, we compute the tail probability past a number of different values for r. Figure 2 plots these pairs (r, t). To generate these pairs we evaluated and $r = vt^{1/2}$, $r = \frac{vt}{\sqrt{\ln t}}$, $r = vt$, where v is varied from 10^{-3} to 10. We exclude pairs of r and t for which $r > t$ (shown as a red line in the figure). Additionally, we only use $r \geqslant 3$ to exclude short-time lattice effects.

We numerically evolve the probability mass function of a random walk by direct implementation of Eq. (2) for a $(t/2 + 1) \times (t/2 + 1)$ lattice with origin in the center out to time $t = 10\,000$. We choose this lattice size to optimize the memory usage of our high-performance computing cluster. As this will necessitate probability mass leaving our simulation volume, we use absorbing boundary conditions to collect this probability mass. The effects of the absorbing boundary condition on the tail probability are negligible. We average our data over 500 realizations of $\boldsymbol{\xi}$ for each ν.

IV. RESULTS

As shown in Fig. 3, the mean of the log of the tail probability, $\mathbb{E}_\nu[\ln(\mathbb{P}^{\boldsymbol{\xi}}(|\vec{S}(t)| \geqslant r))]$, yields the first-order Gaussian behavior as $t \to \infty$ such that [21]

$$\mathbb{E}_\nu[\ln(\mathbb{P}^{\boldsymbol{\xi}}(|\vec{S}(t)| \geqslant r))] \approx -\frac{r^2}{t}. \tag{7}$$

We expect this Gaussian behavior because the average environment is homogeneous, as in classical diffusion.

In Fig. 4 (top) we plot the scaled variance $\frac{t^2}{r^2\lambda_{\text{ext}}}\text{Var}_\nu[\ln(\mathbb{P}^{\boldsymbol{\xi}}(|\vec{S}(t)| \geqslant r))]$ for every r, t, and ν as a function of time, t. We plot the median value of the scaled variance in each of 50 logarithmically spaced bins in time, for each choice of ν, colored by the value of λ_{ext}. We plot the median value of all data in black. The scaling factor $t^2/r^2\lambda_{\text{ext}}$ collapses nearly all of the data onto a single constant as a function of time. Thus, the large deviation regime in which $r \propto t$ will result in a constant-in-time variance of the tail

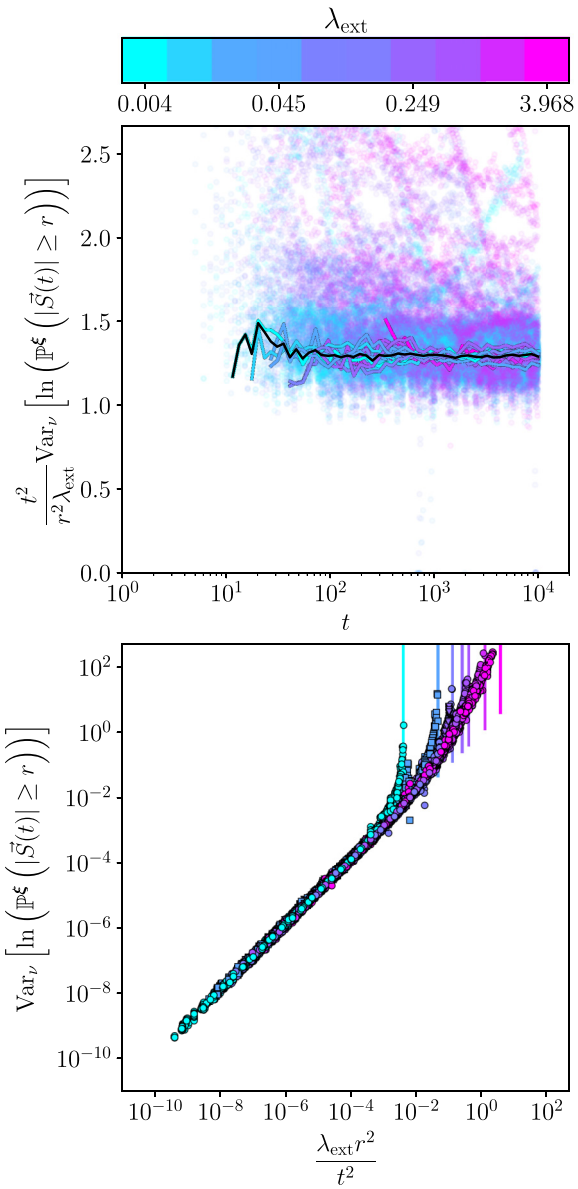

FIG. 4. Universal critical behavior of the tail probability in the large deviation regime. Color gradient encodes the value of λ_{ext} from 0.004 (blue) to 4 (pink). Top: Variance of $\ln\left(\mathbb{P}^\xi(|\vec{S}(t)|\geqslant r)\right)$ as a function of t, normalized by $\lambda_{\text{ext}}r^2/t^2$. The black line plots the median across all ν, calculated as described in the text. The solid colored lines plot the median for each ν. Bottom: Variance of $\ln\left(\mathbb{P}^\xi(|\vec{S}(t)|\geqslant r)\right)$ as a function of $\lambda_{\text{ext}}r^2/t^2$. Markers indicates specific choices of ν: Dirichlet (circles), random-delta (triangles), and the corner distribution (squares). Vertical lines indicate where $r=t$ for each value of λ_{ext}.

probability. Therefore, the critical scaling regime is the large deviation regime. As discussed in Sec. IV A, when $r/t\to 1$, there is nonuniversal, but easily explained, behavior. This data is excluded from the median calculation.

We find that the data collapses onto

$$\text{Var}_\nu[\ln\left(\mathbb{P}^\xi(|\vec{S}(t)|\geqslant r)\right)] = c\lambda_{\text{ext}}\frac{r^2}{t^2} \tag{8}$$

for $r<t$, where we empirically determine $c\approx 1.3$. Note that for $d=1$ RWRE models this prefactor is analytically determined [14]. We replot our data in Fig. 4 (bottom) onto this universal form, which shows that λ_{ext} captures all relevant information about the environment (i.e., the choice of ν).

The parameter λ_{ext} characterizes the stickiness of random walks in the given environment, i.e., how likely two random walks at the same site and same time will remain together. To illustrate, consider the following limits. When the environment is homogeneous in space and time, as in the classical model for diffusion, we recover the SSRW wherein $\xi(\hat{n})=1/4$ for all $\hat{n}\in\boldsymbol{n}$. Trajectories are uncorrelated, and the variance across all samples of ν of a single jump is 0. Thus, $D_{\text{ext}}\to 0$, and $\lambda_{\text{ext}}\to 0$. In contrast, a completely sticky environment has, at each site and time, a jump distribution with unit probability in one random nearest-neighbor direction. In this instance the variance across all samples of ν of a single jump will approach D, and thus $\lambda_{\text{ext}}\to\infty$.

A. Nonuniversal behavior

For a given value of λ_{ext}, as r approaches t we see the transition to nonuniversal behavior in the fluctuations for the tail probability. This behavior is fundamentally a lattice effect driven by the narrowing of the number of possible paths between the origin and sites past r. When $r=t$, there will only be four sites at or past r. Thus, the fluctuations of $\mathbb{P}^\xi(|\vec{S}(t)|=t)$ will be well described as the fluctuations of the sum of four random and independent paths, and so our measured variance should scale linearly with t for large t. When plotting the mean (Fig. 3), this appears as deviations from the Gaussian prediction, and when plotted on our master curve (Fig. 4, bottom), this appears as a deviation to a vertical line at λ_{ext}.

We explicitly compute

$$\mathbb{P}^\xi(|\vec{S}(t)|=t) = \sum_{\hat{n}\in\boldsymbol{n}}\mathbb{P}^\xi(\vec{S}(t)=t\hat{n}) \tag{9}$$

as a sum over the four cardinal paths.

We consider the probability of reaching site $t\hat{n}$ along a cardinal path,

$$\mathbb{P}^\xi(\vec{S}(t)=t\hat{n}) = \prod_{i=1}^{t}\xi_{i\hat{n},i}(\hat{n}), \quad \text{and}$$
$$\ln(\mathbb{P}^\xi(\vec{S}(t)=t\hat{n})) = \sum_{i=1}^{t}\ln\left(\xi_{i\hat{n},i}(\hat{n})\right). \tag{10}$$

Thus, we find the variance for a single site at the end of the cardinal path to be

$$\begin{aligned}\text{Var}_\nu[\ln(\mathbb{P}^\xi(\vec{S}(t)=t\hat{n}))] &= \sum_{i=1}^{t}\text{Var}_\nu[\ln\left(\xi_{i\hat{n},i}(\hat{n})\right)]\\ &= t\,\text{Var}_\nu[\ln\left(\xi_{\vec{x},t}(\hat{n})\right)],\end{aligned} \tag{11}$$

where in the first line we used the fact that $\xi_{\vec{x},t}$ are independent at different lattice sites $(\vec{x},t)$, and in the second line used the property that all $\xi_{\vec{x},t}$ are identically distributed.

To calculate the variance of the tail probability at $r = t$, we need to consider all four cardinal paths to find

$$\begin{aligned}&\mathrm{Var}_\nu[\ln(\mathbb{P}^{\boldsymbol{\xi}}(|\vec{S}(t)| = t))]\\ &= \mathrm{Var}_\nu\left[\ln\left(\sum_{\hat{n}\in\boldsymbol{n}} \mathbb{P}^{\boldsymbol{\xi}}\big(\vec{S}(t) = t\hat{n}\big)\right)\right]\\ &\approx \mathrm{Var}_\nu[\ln(4\mathbb{P}^{\boldsymbol{\xi}}(\vec{S}(t) = t\hat{n}))] \qquad (12)\end{aligned}$$

using the approximation

$$\sum_{\hat{n}\in\boldsymbol{n}} \mathbb{P}^{\boldsymbol{\xi}}(\vec{S}(t) = t\hat{n}) \approx 4\mathbb{P}^{\boldsymbol{\xi}}(\vec{S}(t) = t\hat{n}), \qquad (13)$$

which we expect to be reasonable in the limit that $t \to \infty$, because the variable $\mathbb{P}^{\boldsymbol{\xi}}(\vec{S}(t) = t\hat{n})$ is independent and identically distributed for all $\hat{n} \in \boldsymbol{n}$, except at $t = 0$. Therefore,

$$\begin{aligned}&\mathrm{Var}_\nu[\ln(\mathbb{P}^{\boldsymbol{\xi}}(|\vec{S}(t)| = t))]\\ &\approx \mathrm{Var}_\nu[\ln(4) + \ln(\mathbb{P}^{\boldsymbol{\xi}}(\vec{S}(t) = t\hat{n}))]\\ &= \mathrm{Var}_\nu[\ln(\mathbb{P}^{\boldsymbol{\xi}}(\vec{S}(t) = t\hat{n}))]\\ &= t\,\mathrm{Var}_\nu[\ln(\xi_{\vec{x},t}(\hat{n}))]. \qquad (14)\end{aligned}$$

Thus, the variance of the tail probability when $r = t$ scales linearly with time as $t \to \infty$.

V. CONCLUSION

We have shown in this paper that RWRE models exhibit universal fluctuations of the tail probability in $d = 2$. We find the critical scaling occurs for $r \propto t$, in contrast to the $d = 1$ case for which the critical scaling regime is $r \propto t^{3/4}$. As the large deviation regime is the upper bound on scalings for our model, this means that $d = 2$ RWRE models exhibit universal behavior in *every* scaling. Additionally, the fluctuations of the tail probability decrease in time at every scaling except the critical scaling. Thus, RWRE models in $d = 2$ approach classical behavior at long times in every regime except for the large deviation regime. This results raises the important question of whether or not a critical regime exists in $d > 2$. In the $d = 1$ RWRE case, the critical scaling regime $r \propto t^{3/4}$ can be translated into precise statements about the scaling of the fluctuations in the extreme location at time t (the position of the particle farthest from the origin) and the extreme first passage time at distance L (the shortest time for a particle to reach L). While analogous translations have yet to be done for the $d = 2$ case, the critical scaling regime of $r \propto t$ requires that the analogous fluctuations must have a slower scaling than in $1d$. Thus, one should expect that the extremes, in the asymptotic limit that $t \to \infty$, in $2d$ systems will be more predictable than in $1d$.

A scaling argument in Ref. [21] and unpublished mathematical work by Drillick and Parekh conjecture a critical scaling regime for $d = 2$ RWRE models [32] that differs from the empirically observed large deviation regime. In those works, through a weak disorder one loop RG argument [21] and by studying the tail probability past a line [32], the authors find the critical scaling regime to occur at line positions $\propto t/\sqrt{\ln t}$. This discrepancy is intriguing and will require more work. The fluctuations in the tail probability past a line can be understood as effectively local, since they will be dominated by the fluctuations at the point of the line's closest approach to the origin. However, the tail probability past a circle will always be global, since every point on the circle is equidistant to the origin and thus the fluctuations are not dominated by any single point. One might expect these two measurements to differ by logarithmic corrections. Further work is necessary to resolve this difference: empirical studies of the fluctuations past a line and analytical studies of the fluctuations past a circle.

The critical scaling regime in $d = 1$ relates to the $(1 + 1)d$ KPZ equation. As we have uncovered the $d = 2$ critical scaling regime, it is natural to ask whether it relates to the $(2 + 1)d$ KPZ equation [31,33]. Perhaps a detailed examination of the full distribution of the tail probability will be illuminating. Additionally, it would be valuable to extend the exploration of $d = 2$ RWRE models to cover long-range jump kernels as well as other measurements such as probability to reach a point and probability to reach a line.

ACKNOWLEDGMENTS

We thank Axel Saenz Rodriguez, Ivan Corwin, Hindy Drillick, and Pierre Le Doussal for discussion. The authors acknowledge Research Advanced Computing Services (RACS) at the University of Oregon for providing computing resources that have contributed to the research results reported within this publication. This work was funded by a W. M. Keck Foundation Science and Engineering grant on "Extreme Diffusion."

DATA AVAILABILITY

The data that support the findings of this article are not publicly available upon publication because it is not technically feasible and/or the cost of preparing, depositing, and hosting the data would be prohibitive within the terms of this research project. The data are available from the authors upon reasonable request.

[1] A. Einstein, Über die von der molekularkinetischen theorie der Wärme geforderte bewegung von in ruhenden flüssigkeiten suspendierten teilchen [AdP 17, 549 (1905)], Ann. Phys. **517**, 182 (2005).

[2] A. Einstein, Zur theorie der Brownschen bewegung [AdP 19, 371 (1906)], Ann. Phys. **517**, 248 (2005).

[3] A. Einstein, Theoretische bemerkungen Über die Brownsche bewegung, Z. Elektrochem. Angew. Phys. Chem. **13**, 41 (1907).

[4] K. Reynaud, Z. Schuss, N. Rouach, and D. Holcman, Why so many sperm cells? Commun. Integr. Biol. **8**, e1017156 (2015).

[5] S. D. Lawley, Distribution of extreme first passage times of diffusion, J. Math. Biol. **80**, 2301 (2020).

[6] K. Basnayake, D. Mazaud, A. Bemelmans, N. Rouach, E. Korkotian, and D. Holcman, Fast calcium transients in dendritic spines driven by extreme statistics, PLoS Biol. **17**, e2006202 (2019).

[7] M. J. Keeling, M. E. J. Woolhouse, D. J. Shaw, L. Matthews, M. Chase-Topping, D. T. Haydon, S. J. Cornell, J. Kappey, J. Wilesmith, and B. T. Grenfell, Dynamics of the 2001 UK foot and mouth epidemic: Stochastic dispersal in a heterogeneous landscape, Science **294**, 813 (2001).

[8] L. Hufnagel, D. Brockmann, and T. Geisel, Forecast and control of epidemics in a globalized world, Proc. Natl. Acad. Sci. USA **101**, 15124 (2004).

[9] F. Iannelli, A. Koher, D. Brockmann, P. Hövel, and I. M. Sokolov, Effective distances for epidemics spreading on complex networks, Phys. Rev. E **95**, 012313 (2017).

[10] M. Balázs, F. Rassoul-Agha, and T. Seppäläinen, The random average process and random walk in a space-time random environment in one dimension, Commun. Math. Phys. **266**, 499 (2006).

[11] G. Barraquand and I. Corwin, Random-walk in beta-distributed random environment, Probab. Theory Relat. Fields **167**, 1057 (2017).

[12] A. Pacheco-Pozo and I. M. Sokolov, Large deviations in continuous-time random walks, Phys. Rev. E **103**, 042116 (2021).

[13] J. B. Hass, A. N. Carroll-Godfrey, I. Corwin, and E. I. Corwin, Anomalous fluctuations of extremes in many-particle diffusion, Phys. Rev. E **107**, L022101 (2023).

[14] J. B. Hass, H. Drillick, I. Corwin, and E. I. Corwin, Extreme diffusion measures statistical fluctuations of the environment, Phys. Rev. Lett. **133**, 267102 (2024).

[15] J. Hass, H. Drillick, I. Corwin, and E. Corwin, Universal Kardar-Parisi-Zhang fluctuations for moderate deviations of random walks in random environments, Phys. Rev. E **113**, 014136 (2026).

[16] H. Kesten, M. V. Kozlov, and F. Spitzer, A limit law for random walk in a random environment, Compos. Math. **30**, 145 (1975).

[17] J.-P. Bouchaud and A. Georges, Anomalous diffusion in disordered media: Statistical mechanisms, models and physical applications, Phys. Rep. **195**, 127 (1990).

[18] J. P Bouchaud, A. Comtet, A. Georges, and P. Le Doussal, Classical diffusion of a particle in a one-dimensional random force field, Ann. Phys. **201**, 285 (1990).

[19] A. Pisztora and T. Povel, Large deviation principle for random walk in a quenched random environment in the low speed regime, Ann. Probab. **27**, 1389 (1999).

[20] L. Defaveri and E. Barkai, Diffusion in quenched random environments: Reviving Laplace's first law of errors, arXiv:2501.05585.

[21] P. Le Doussal, and T. Thiery, Diffusion in time-dependent random media and the Kardar-Parisi-Zhang equation, Phys. Rev. E **96**, 010102 (2017).

[22] G. Barraquand, and P. Le Doussal, Moderate deviations for diffusion in time dependent random media, J. Phys. A: Math. Theor. **53**, 215002 (2020).

[23] J. B. Hass, I. Corwin, and E. I. Corwin, First-passage time for many-particle diffusion in space-time random environments, Phys. Rev. E **109**, 054101 (2024).

[24] S. Parekh, Hierarchy of KPZ limits arising from directed random walk models in random media, arXiv:2401.06073.

[25] S. Das, H. Drillick, and S. Parekh, Multiplicative SHE limit of random walks in space-time random environments, Probab. Theory Relat. Fields (2024).

[26] J. Hass, Super-universal behavior of outliers diffusing in a space-time random environment, arXiv:2505.01533.

[27] M. Kardar, G. Parisi, and Y.-C. Zhang, Dynamic scaling of growing interfaces, Phys. Rev. Lett. **56**, 889 (1986).

[28] K. A. Takeuchi, and M. Sano, Universal fluctuations of growing interfaces: Evidence in turbulent liquid crystals, Phys. Rev. Lett. **104**, 230601 (2010).

[29] S. Prolhac and H. Spohn, Height distribution of the Kardar-Parisi-Zhang equation with sharp-wedge initial condition: Numerical evaluations, Phys. Rev. E **84**, 011119 (2011).

[30] M. Kardar and Y.-C. Zhang, Scaling of directed polymers in random media, Phys. Rev. Lett. **58**, 2087 (1987).

[31] T. Halpin-Healy, (2+1)-dimensional directed polymer in a random medium: Scaling phenomena and universal distributions, Phys. Rev. Lett. **109**, 170602 (2012).

[32] H. Drillick and S. Parekh, Random walks in space-time random media in all spatial dimensions: The full subcritical fluctuation regime, arXiv:2510.22155.

[33] T. Halpin-Healy, Extremal paths, the stochastic heat equation, and the three-dimensional Kardar-Parisi-Zhang universality class, Phys. Rev. E **88**, 042118 (2013).